MgO-Based Epitaxial Magnetic Tunnel Junctions Using Fe-V Electrodes

Frédéric Bonell[1], Stéphane Andrieu[1], François Bertran[2], Patrick Lefèvre[2], Amina Taleb Ibrahimi[2], Etienne Snoeck[3], Coriolan-Viorel Tiusan[1], and François Montaigne[1]

[1]Institut Jean Lamour, UMR CNRS 7198, Université H. Poincaré, Nancy 54506, France
[2]Synchrotron SOLEIL, Gif-sur-Yvette Cedex 91192, France
[3]CEMES-CNRS, Toulouse Cedex 31055, France

To examine the influence of the barrier quality in fully epitaxial Fe/MgO/Fe(001) magnetic tunnel junctions (MTJs), we propose to use Fe-V alloys as magnetic electrodes. This leads to a reduced misfit with MgO. We actually observe, by high-resolution electron microscopy (HREM) and local strain measurements, that the misfit dislocations density in the MgO barrier is lower when it is grown on Fe-V(001). This improvement of the crystalline quality of the MgO barrier actually leads to a significant increase of the tunnel magneto-resistance (TMR), despite the loss of spin polarization (SP) in these alloys, which was measured by spin-polarized X-ray photoelectron spectroscopy (SR-XPS).

Index Terms—**Dislocation, epitaxial magnetic tunnel junction, Fe-V alloy, MgO, spin polarization.**

I. Introduction

THE symmetry-dependent filtering of electronic Bloch waves by an epitaxial tunnel barrier [1] was first evidenced in MgO-based magnetic tunnel junctions (MTJs) [2], [3]. When a thin MgO(001) layer is coupled with magnetic BCC electrodes, this effect leads to the so-called giant tunnel magneto-resistance (giant TMR). In the asymptotic regime, corresponding to a thick MgO barrier (typically 2.5 nm), one can roughly consider that the only tunneling electrons propagate perpendicularly to interfaces along the [001] direction of the crystal (electrons with $k_{||} = 0$). This corresponds to the Δ direction of the reciprocal lattice. Then, the large TMR arises from: 1) the half-metallicity of BCC Fe with respect to the Δ_1 symmetry Bloch states; and 2) the small decay rate of Δ_1 states within the MgO barrier compared to other existing electronic symmetries (Δ_5, Δ_2, and $\Delta_{2'}$) [1].

Improving the characteristics of MTJs (larger TMR, lower resistance, and lower noise) remains a major challenge for technological developments. Concerning the TMR, this improvement was gradually obtained by using materials that have an increasingly high spin polarization (SP) of the Δ bands at the Fermi level: initially Fe [2], then FeCo and BCC Co [4]. In contrast, the present work proposes an alternative way by focusing on the filtering efficiency of the MgO barrier. The optimization of this filtering efficiency may lead to both larger TMR and potentially lower noise.

Up to now, the reported TMR values remain one order of magnitude below the theoretical predictions. Many reasons may explain this discrepancy between theory and experiments. As the calculations were performed assuming perfect crystalline arrangement in both Fe and MgO and at the interfaces, looking closely to the possible defects in the whole grown structure is obvious. Several kinds of defects were clearly identified, like crystalline defects in the Fe layers and in the MgO barrier,and possible C and O pollution at the Fe/MgO interfaces. The crystalline defects in the Fe layers, and especially on the top Fe layer grown on the MgO barrier, are eliminated by annealing the stacking after the growth [5]. This step clearly increases the TMR from around 100% for as-grown samples to 180% after annealing. The second point is the chemical quality of the interface. We proposed a technique to eliminate the C contamination at the interface [6], [7]. Certainly, the most discussed source of interfacial pollution is the presence of oxygen at the interface due to the MgO growth itself [8]. Indeed, several groups have shown by calculations that the presence of oxygen at the interface leads to detrimental effects on the TMR [9], [10]. We recently studied this effect by doping the Fe/MgO interface with a controlled amount of oxygen from 0.1 to 2 ML [11], [12]. Surprisingly, we found that the TMR was reduced by only 20% with one oxygen monolayer doping compared to an undoped stacking. For this reason, we now focus on the crystalline quality of the MgO barrier. For instance, defects like O vacancies [13], [14] were taken into account in calculation, leading to detrimental effect on the TMR [15]. However, it is also well known that epitaxial barriers contain defects due to the lattice mismatch with Fe (3.9%). In particular, interfacial misfit dislocations appear during the plastic relaxation of MgO on Fe(001) after deposition above five to six atomic planes [16]–[18]. However, 2.5-nm-thick MgO barriers are needed to achieve high TMR ratios [2] and consequently contain dislocations. To our knowledge, the influence of these dislocations on tunneling has not been addressed yet.

A way to decrease the dislocation density is to reduce the strain and, therefore, the misfit between the MgO barrier and the supporting magnetic electrode. To obtain a large TMR, one has to choose an appropriate electrode combining several characteristics. First, its lattice parameter must be close to the one of MgO. Second, a BCC structure is needed in order to keep the sensitivity of tunneling to states with Δ symmetry. Third, the SP of the material has to be large, in particular the SP of Δ bands. Alloying with Fe is a way to keep a BCC structure and an electronic structure close to the Fe one. Moreover, one can, in principle, adjust the stoichiometry of the alloy so as to engineer the crystalline/electronic structure [19], [20]. We thus used BCC Fe-V electrodes, which are known to have a larger lattice parameter compared to Fe.

Manuscript received March 06, 2009. Current version published September 18, 2009. Corresponding author: F. Bonell (e-mail: bonell@lpm.u-nancy.fr).

Color versions of one or more of the figures in this paper are available online at http://ieeexplore.ieee.org.

Digital Object Identifier 10.1109/TMAG.2009.2022644

The structural characterization of Fe-V films, MgO barriers, and the whole MTJ stacking are reported in Section III-A. Measurements of the Fe-V alloys SP when covered with MgO are presented in Section III-B. The influence of Fe-V when used as an electrode in MTJs will be discussed in Section III-C.

II. Experimental Details

The growth of single-crystal multilayers on MgO(001) was performed by molecular beam epitaxy operating with a base pressure of 8×10^{-9} Pa. MgO(001) substrates were outgassed at 875 K, and an additional 7-nm-thick MgO layer was grown at 725 K in order to improve the quality of the substrate surface and to avoid the diffusion of residual carbon during subsequent annealing [6]. Fe-V alloys were grown by co-evaporation of Fe and V. Fe was evaporated in a Knudsen cell heated at 1523 K. V was evaporated by electron beam heating at different evaporation rates, depending on the desired concentration. Evaporation rates were calibrated by using quartz microbalances. The composition of the alloys was checked *a posteriori* by X-ray photoelectron spectroscopy (XPS), using a standard $\mathrm{Al}-\mathrm{K}\alpha$ source. The films were then annealed 20 min around 825 K in order to improve their homogeneity and to obtain very flat surfaces. The stacking used for magneto-transport and high-resolution electron microscope (HREM) measurements was Fe-V (50 nm)/MgO (2.5 nm)/Fe-V (18 nm)/Co (20 nm)/Au (10 nm). The detailed preparation of fully epitaxial MTJs is described in [11]. The preparation of specimens for TEM studies is described in [21]. In addition to standard cross-section imaging, a mapping of local strain was performed so as to visualize the dislocations, using the phase method proposed in [22].

Spin-resolved X-ray photoelectron spectroscopy (SR-XPS) was carried out on 50-nm-thick Fe-V films covered with 2 ML of MgO. MgO was deposited by evaporating a stoichiometric source by electron beam heating. The thickness of the MgO over-layer was precisely controlled by monitoring RHEED intensity oscillations during the growth. Samples were grown in the Institut Jean Lamour of Nancy, France, and were stocked under N_2 atmosphere before SR-XPS measurements at SOLEIL Synchrotron. After reintroduction under ultra-high vacuum, they were annealed 2 h at 423 K in order to desorb eventual contaminants. The photoemission spectra were recorded at room temperature. The sample was magnetized applying a field around 100 Oe applied in the [100] in-plane easy axis (as checked by VSM) and were measured at remanence. The remanent magnetization was 100%, 98%, and 97% of the saturation magnetization for Fe, $\mathrm{Fe}_{0.9}\mathrm{V}_{0.1}$, and $\mathrm{Fe}_{0.8}\mathrm{V}_{0.2}$, respectively. In order to compensate eventual detector asymmetries, the spectra were measured for both opposite directions of magnetization. Linearly p-polarized light with photon energy of $h = 60$ eV was used. At this energy, the ratio of the oxygen $2p$ and iron $3d$ photoionization cross sections is quite low, as well as the attenuation rate of emitted photoelectrons. This allows efficiently probing the Fe density of states (DOS) in the band-gap of MgO. The incoming beam had an incident angle of 45°. The plane of incidence was defined by the [100] in-plane and the [001] surface normal crystallographic directions of the films. Photoelectrons emitted with their wave vector k along the surface normal were detected by a hemispherical analyzer coupled to a Mott detector, with an angular acceptance of $\pm 1.8°$. In this geometry, dipole selection rules ensure that the direct transitions between Δ bands are mainly probed [23]. The total resolution in energy was set to 170 meV. The resolution in k deduced from the photon energy and angular acceptance was $\Delta k_{||} = \pm 0.13\ \mathrm{\AA}^{-1}$.

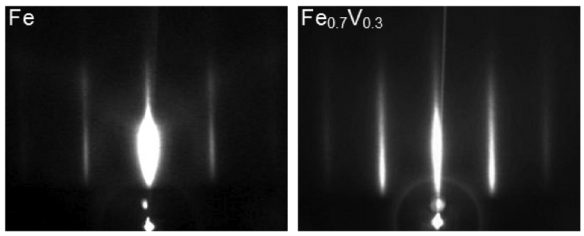

Fig. 1. RHEED patterns of Fe(001) and $\mathrm{Fe}_{0.7}\mathrm{V}_{0.3}(001)$ surfaces, previously annealed at 825 K. The electron beam is aligned with the [100] crystallographic direction of the surface lattice.

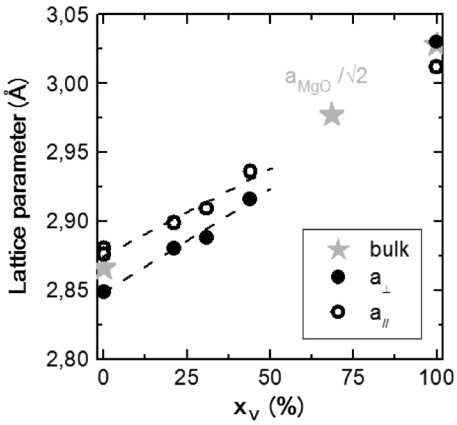

Fig. 2. In-plane (empty circles) and out-of-plane (filled circles) lattice parameters of 50-nm-thick Fe-V films grown on MgO(001), measured by XRD. Stars are the lattice parameters of bulk Fe and V and the one of MgO divided by $\sqrt{2}$.

III. Results

A. Structural Characterizations

Electron and X-ray diffraction (XRD) analysis of Fe-V films capped with 1 nm of MgO show that these alloys are still BCC at $x = 50\%$, with x the atomic concentration of vanadium. No surface reconstruction is observed by RHEED (Fig. 1). Fig. 2 shows XRD measurements of the crystalline parameters (in-plane and out-of-plane). Their dependence with x is almost linear and can therefore be described by a Vegard's law. Moreover, 50-nm-thick films remain slightly tetragonalized. Because of the strain in tension due to the MgO(001) substrate, the average in-plane lattice parameter is slightly larger than the out-of-plane one.

The plastic relaxation of MgO grown on Fe-V was studied by measuring the variation of the in-plane lattice spacing by RHEED during the MgO deposition. Experiments were performed in anti-Bragg geometry with the electron beam aligned with the [110] crystallographic direction of the MgO surface lattice. Profiles perpendicular to the diffraction rods were recorded and fitted with lorentzian line shapes. This procedure allows extracting the variations of the diffracted intensity and the distance between the rods, the latter being inversely proportional to the

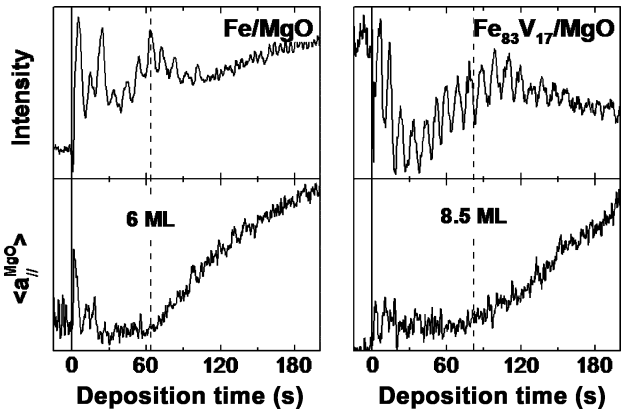

Fig. 3. RHEED intensity oscillations and evolution of the in-plane lattice spacing in the [110]MgO direction, measured during the growth of MgO(001) on (left) Fe and (right) $\mathrm{Fe_{0.8}V_{0.2}}$. The critical thickness for plastic relaxation is indicated by dashed lines.

in-plane lattice spacing of the topmost atomic plane [18], [24]. Results for MgO grown on Fe(001) and $\mathrm{Fe_{0.8}V_{0.2}}(001)$ are reported in Fig. 3. In both cases, the diffracted intensity is found to oscillate. This is indicative of a layer-by-layer growth, each maximum corresponding to the completion of an MgO atomic plane. The lattice spacing of the growing *topmost* MgO layer is constant during the initial stages of deposition, then increases continuously. These two regimes are characteristic of a pseudomorphic growth followed by a sudden relaxation of the accumulated elastic energy by the creation of dislocations and/or a change of the growth mode from 2D to 3D. The critical thickness for plastic relaxation is between 5 and 6 ML on Fe(001) and reaches 8–9 ML on $\mathrm{Fe_{0.8}V_{0.2}}(001)$.

This increase of the critical thickness for plastic relaxation is confirmed by HRTEM. Fig. 4(a) shows a low-magnification HR-TEM image of an $\mathrm{Fe_{0.8}V_{0.2}/MgO/Fe/Co/Au}$ epitaxial MTJ. Sharp interfaces and a continuous MgO barrier can be seen. Fig. 4(b) shows a map of strain around the barrier. At the $\mathrm{Fe_{0.8}V_{0.2}/MgO}$ and MgO/Fe interfaces, strain is localized in the vicinity of dislocations, which appear as hot spots. Obviously, the dislocation density is lower at the $\mathrm{Fe_{0.8}V_{0.2}/MgO}$ interface compared to the MgO/Fe top interface. This confirms that the misfit with MgO is actually reduced, leading to an improvement of the crystalline quality of the barrier and the interfaces.

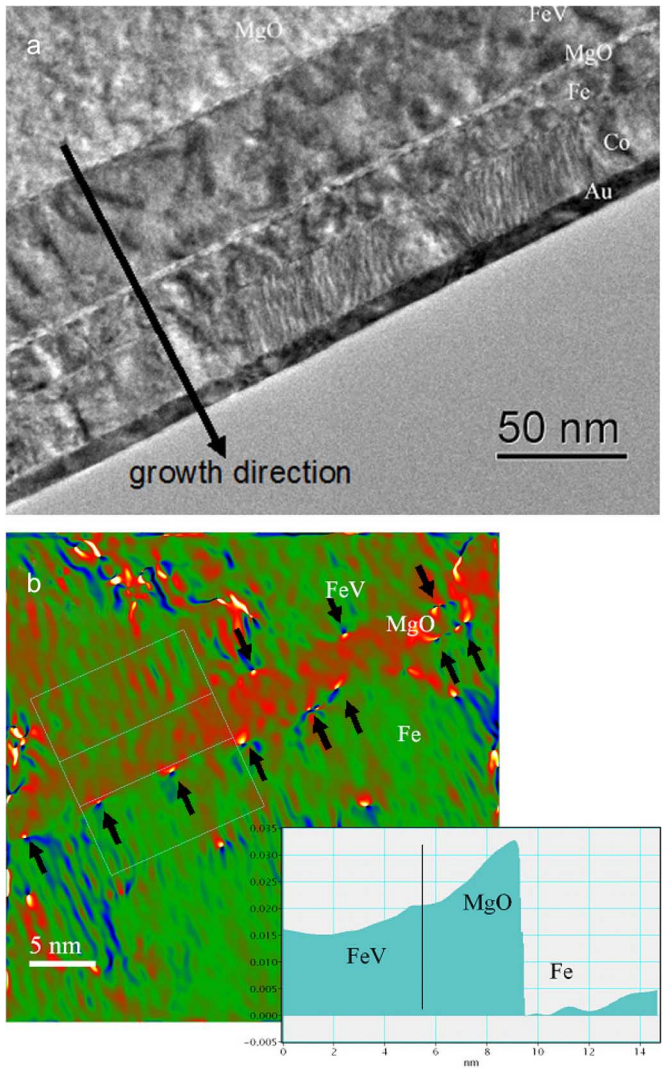

Fig. 4. (a) Low-magnification TEM image of an epitaxial $\mathrm{MgO//Fe_{0.8}V_{0.2}/MgO/Fe/Co/Au}$ MTJ in the Fe[110] zone-axis. (b) Map of strain in atomic planes normal to the interface [(200)-MgO and (110)-Fe]. Misfit dislocations at both sides of the barrier are indicated by arrows. Their density is higher at the MgO/Fe interface than at the Fe-V/MgO one. The graph shows a profile of strain across the barrier, integrated in the zone delimited by the white borders. Values are given in %, taking the Fe(110) layer as reference.

B. Magnetism of Fe-V Alloys Covered With MgO

Up to now, the SP of Fe-V, and *a fortiori* the polarization of MgO covered Fe-V alloys, has not been measured.

The electronic structure of Fe-rich disordered alloys has been investigated by means of *ab initio* calculations. Johnson's calculations explain the drop of the magnetic moment upon vanadium addition [19], which arises from the fact that the minority DOS remains almost unchanged, whereas the majority one follows a rigid band behavior. This underlies a peculiar behavior of the DOS at the Fermi level $(\mathrm{E_F})$. The peak related to majority d states lying under $\mathrm{E_F}$ gradually moves toward and above $\mathrm{E_F}$ when the amount of V increases. Although the total magnetic moment decreases, one therefore expects an increase of the polarization at $\mathrm{E_F}$ for moderate amounts of V (around 30%), the maximum SP being observed when the peak of majority d states is exactly at $\mathrm{E_F}$ [20]. However, the situation may be not so direct because bands are not rigid and distort upon vanadium addition.

SR-XPS experiments are potentially able to settle this question by directly measuring the spin polarization at $\mathrm{E_F}$, a crucial point in the interpretation of spin-polarized tunneling experiments. Moreover, tunneling through epitaxial MgO(001) tunnel barriers is known to be governed by electronic states with Δ symmetry, i.e. states with a predominant s character [1]. The most relevant information is therefore the *SP of* Δ *states*, which has not been theoretically studied yet. As explained in Section II, valuable information about the Δ bands can be obtained by a proper choice of the photoemission experimental configuration.

In order to illustrate the drop of the magnetic moment in Fe-V alloys, we show in Fig. 5 its dependence on the concentration of vanadium, measured with VSM. The measured moment of Fe is

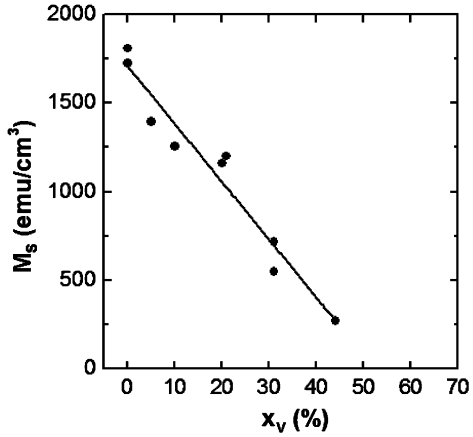

Fig. 5. Saturation magnetization of Fe-V alloys versus vanadium content, measured with VSM.

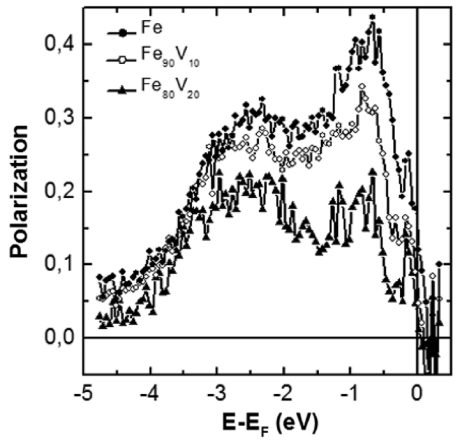

Fig. 6. Spin polarization of Fe-V alloys covered with MgO (2 ML) measured by SR-XPS ($\mathrm{h}\nu = 60$ eV, Sherman function $\mathrm{S} = 0.12$).

about 1750 emu/cm^3. This value drops almost linearly upon V addition. By extrapolation, the moment falls down to zero near 52% of V.

We investigated the SP of Fe-V films covered with 2 ML of MgO. The results for $x = 0\%$, $x = 10\%$, and $x = 20\%$ are shown in Fig. 6. Below 3.5 eV from $\mathrm{E_F}$, the polarization falls down to nearly zero because nonpolarized states from the valence band of MgO are probed in addition to Fe-V ones. For all the investigated samples, SP maxima are observed at 2.5 and 0.7 eV below $\mathrm{E_F}$. They originate from maxima in the majority spins DOS. No significant singularity due to vanadium addition appears in this range of concentrations. This means that the characteristic features of the Fe DOS are almost conserved in Fe-V alloys. SR-XPS measurements on Fe/MgO(001) carried out in similar experimental conditions were reported in [22]. Following this study, the features at 2.5 and 0.7 eV can be respectively assigned to $\Delta_5^{\uparrow} \rightarrow \Delta_1^{\uparrow}$ and $\Delta_1^{\uparrow} \rightarrow \Delta_1^{\uparrow}$ direct transitions. A third peak in the SP is observed at 0.15 eV below $\mathrm{E_F}$. At the moment, interpreting this feature in terms of interband transitions would need further theoretical investigation of the band structure. The maximum SP is measured at around 0.7 eV for all samples. It reaches 44% for the Fe/MgO interface, in fair agreement with previous measurements. This value drops to 34% and 22% for the $\mathrm{Fe_{0.9}V_{0.1}/MgO}$ and $\mathrm{Fe_{0.8}V_{0.2}/MgO}$ interfaces, respectively. Importantly, the SP at $\mathrm{E_F}$ continuously decreases as well when increasing the V content.

In partial summary, growing MgO on Fe-V(001) instead of Fe(001) allows to reduce the misfit dislocations density. These dislocations appear during the plastic relaxation of MgO, which is strained on Fe. Improving the MgO growth leads to a final stacking closer to the ideal structure expected to provide a huge TMR. However, SR-XPS measurements show that the SP of states with Δ symmetry drops continuously when increasing the vanadium concentration. Since tunneling in epitaxial MgO-based MTJs is governed by the Δ states, this should in principle be detrimental for the TMR.

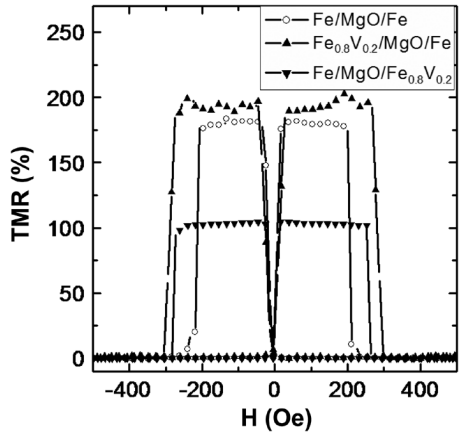

Fig. 7. TMR of various Fe-V/MgO (2.5 nm)/Fe-V(001) MTJs versus applied magnetic field (RT, applied voltage: 10 mV). The TMR is defined as $(R(H) - R_P)/R_P$, where R_P is the resistance in the parallel alignment of magnetizations. MgO grown on Fe-V provides larger TMR than MgO grown on Fe.

C. TMR of Epitaxial MTJs With Fe-V Electrodes

The magneto-transport experiments were performed on MTJ stacks with MgO barrier thickness of 2.5 nm. This corresponds to the asymptotic regime where the dominant propagating wave functions have a wave vector normal to the interfaces. In this regime, tunneling is dominated by electronic states with Δ_1 symmetry, i.e. those with the smaller attenuation rate within the MgO. The TMR of several MTJs versus the applied magnetic field H is shown in Fig. 7. Measurements are carried out at RT, with an applied bias of 10 mV. The quantity $\mathrm{TMR}(H)$ is defined as $(R(H) - R_P)/R_P$, where R_P is the resistance of the MTJ when the magnetization of electrodes are in parallel alignment. The high TMR plateaus in $\mathrm{TMR}(H)$ curves correspond to the antiparallel configuration of magnetization (high resistance state).

The TMR in Fe/MgO/Fe MTJs reaches the state-of-the-art value of 180%. In contrast, a TMR of 100% is measured in $\mathrm{Fe/MgO/Fe_{0.8}V_{0.2}}$ MTJs. Such a difference was expected, having in view the lower SP of Δ bands at $\mathrm{E_F}$ in $\mathrm{Fe_{0.8}V_{0.2}}$. Note that the MgO barrier in both MTJs are identical since both were grown on a bottom Fe(001) electrode.

The TMR in $\mathrm{Fe_{0.8}V_{0.2}/MgO/Fe}$ reaches 200%, which is twice the TMR in $\mathrm{Fe/MgO/Fe_{0.8}V_{0.2}}$. This means that the growth sequence actually has strong consequences on tunneling.

Furthermore, the TMR is even larger than in Fe/MgO/Fe. Therefore, it is clear that the better crystalline quality of the barrier grown on $Fe_{0.8}V_{0.2}(001)$ is highly beneficial to the TMR, despite a low SP in $Fe_{0.8}V_{0.2}$.

According to this result, it is clear that an optimum TMR in Fe-V/MgO/Fe MTJs should be obtained for a precise vanadium concentration by finding the best compromise between the structural coherency and the loss of magnetic performances. We actually observed that the TMR reaches a maximum value of 240% for a 10% V concentration.

Reducing the misfit between the MgO barrier and the supporting electrode obviously leads to a lower density of misfit dislocations. Dislocations disturb the structural coherency at interfaces and certainly introduce additional conduction channels detrimental for the TMR. In addition, the plastic relaxation is known to favor the apparition of roughness. Consequently, reducing the misfit is a way to improve the interfaces *on both sides* of the barrier. Last, we must mention that oxygen vacancies were evidenced in both textured MgO grown on GaAs/Fe(001) [13] and epitaxial MgO grown on GaAs(001) [14]. Although not yet evidenced in MgO grown on MgO/Fe(001), their presence is highly suspected. Their detrimental effect on the TMR has been proven by theoretical studies [15]. These vacancy defects were ascribed to compressive strain from the MgO/Fe lattice mismatch, accommodated as the MgO grows [13]. Therefore, a reduction of these defects may also contribute to the large TMR in $Fe_{0.8}V_{0.2}/MgO/Fe$ MTJs.

IV. Conclusion

We reported here a thorough study of MgO-based epitaxial MTJs with Fe-V electrodes. The structure, the magnetism, and the magneto-transport properties of the multilayer stacking were investigated. XRD confirms that the lattice parameter of BCC Fe-V alloys is larger than the one of Fe, and the misfit with MgO is therefore lower. We showed by RHEED that the critical thickness for plastic relaxation of MgO increases from 5–6 ML when grown on Fe(001), and to 8–9 ML when grown on $Fe_{0.8}V_{0.2}(001)$. HR-TEM images confirm that the density of misfit dislocations is much lower at the Fe-V/MgO interface than at the MgO/Fe one. Growing MgO on Fe-V alloys is therefore a way to improve the crystalline quality of the barrier. However, regarding their magnetic properties, Fe-V alloys are, in principle, less interesting than Fe for obtaining a large TMR in MgO-based MTJs. In agreement with the literature, their magnetic moment drops linearly when increasing the vanadium content. High-resolution SR-XPS measurements of MgO covered Fe-V films allowed us to investigate the SP of bands with mainly Δ symmetry, crucial in tunneling. The SP is found to continuously decrease upon vanadium addition, in particular near E_F. When used as a *top* electrode, $Fe_{0.8}V_{0.2}$ lowers the TMR of MTJs because of its lower SP compared to Fe. However, when used as a *bottom* electrode in $Fe_{0.8}V_{0.2}/MgO/Fe$ MTJs, TMR larger than in Fe/MgO/Fe MTJs was reached. Consequently, improving the barrier quality by reducing the misfit with the supporting electrode induces strong beneficial effects on the TMR. We ascribe this to a better symmetry filtering of the barrier. In principle, an optimum TMR in Fe-V/MgO/Fe MTJs should be obtained for a precise vanadium concentration by finding the best compromise between the structural coherency and the lost of magnetic performances.

Our study implies that a material/stacking presenting a high SP and a small misfit with MgO should provide record TMR values.

Acknowledgment

The authors acknowledge financial support from the French CNRS and CEA "METSA" network.

References

[1] W. H. Butler, X.-G. Zhang, T. C. Schulthess, and J. M. MacLaren, *Phys. Rev. B*, vol. 63, p. 054416, 2001.
[2] S. Yuasa, T. Nagahama, A. Fukushima, Y. Suzuki, and K. Ando, *Nature Mater.*, vol. 3, p. 868, 2004.
[3] S. S. P. Parkin, C. Kaiser, A. Panchula, P. M. Rice, B. Hughes, M. Samant, and S.-H. Yang, *Nature Mater.*, vol. 3, p. 862, 2004.
[4] S. Yuasa, T. Katayama, T. Nagahama, A. Fukushima, H. Kubota, Y. Suzuki, and K. Ando, *Appl. Phys. Lett.*, vol. 87, p. 222508, 2005.
[5] C. Tiusan, J. Faure-Vincent, C. Bellouard, M. Hehn, E. Jouguelet, and A. Schuhl, *Phys. Rev. Lett.*, vol. 93, p. 106602, 2004.
[6] M. Sicot, S. Andrieu, C. Tiusan, F. Montaigne, and F. Bertran, *J. Appl. Phys.*, vol. 99, p. 08D301, 2006.
[7] C. Tiusan, M. Sicot, J. Faure-Vincent, M. Hehn, C. Bellouard, F. Montaigne, S. Andrieu, and A. Shuhl, *J. Phys.: Condens. Matter*, vol. 18, pp. 941–956, 2006.
[8] H. L. Meyerheim, R. Popescu, J. Kirschner, N. Jedrecy, M. Sauvage-Simkin, B. Heinrich, and R. Pinchaux, *Phys. Rev. Lett.*, vol. 87, p. 076102, 2001.
[9] X. G. Zhang, W. H. Butler, and A. Bandyopadhyay, *Phys. Rev. B*, vol. 68, p. 092402, 2003.
[10] C. Heiliger, P. Zahn, and I. Mertig, *J. Magn. Magn. Mater.*, vol. 316, p. 478, 2007.
[11] F. Bonell, A. M. Bataille, S. Andrieu, C. Tiusan, B. Kierren, G. Lengaigne, and D. Lacour, *Eur. Phys. J. Appl. Phys.*, vol. 43, pp. 357–361, 2008.
[12] F. Bonell, S. Andrieu, A. M. Bataille, C. Tiusan, and G. Lengaigne, *Phys. Rev. B*, vol. 79, p. 224405, 2009.
[13] P. G. Mather, J. C. Read, and R. A. Buhrman, *Phys. Rev. B*, vol. 73, p. 205412, 2006.
[14] S. Guezo, P. Turban, C. Lallaizon, J. C. Le Breton, P. Schieffer, B. Lepine, and G. Jezequel, *Appl. Phys. Lett.*, vol. 93, p. 172116, 2008.
[15] J. P. Velev, K. D. Belaschenko, S. S. Jaswal, and E. Y. Tsymbal, *Appl. Phys. Lett.*, vol. 90, p. 072502, 2007.
[16] J.-L. Vassent, M. Dynna, A. Marty, B. Gilles, and G. Patrat, *J. Appl. Phys*, vol. 80, p. 5727, 1996.
[17] C. Tiusan, F. Greullet, M. Hehn, F. Montaigne, S. Andrieu, and A. Schuhl, *J. Phys.: Condens. Matter*, vol. 19, p. 165201, 2007.
[18] M. Klaua, D. Ulmann, J. Barthel, W. Wulfhekel, J. Kirschner, R. Urban, T. L. Monchesky, A. Enders, J. F. Cochran, and B. Heinrich, *Phys. Rev. B*, vol. 64, p. 134411, 2001.
[19] D. D. Johnson, F. J. Pinski, and J. B. Staunton, *J. Appl. Phys.*, vol. 61, p. 3715, 1987.
[20] J. P. Renard, P. Bruno, R. Megy, B. Bartenlian, P. Beauvillain, C. Chappert, C. Dupas, E. Kolb, M. Mulloy, P. Veillet, and E. Velu, *Phys. Rev. B*, vol. 51, p. 12821, 1995.
[21] F. Greullet, E. Snoeck, C. Tiusan, M. Hehn, D. Lacour, O. Lenoble, C. Magen, and L. Calmels, *Appl. Phys. Lett.*, vol. 92, p. 053508, 2008.
[22] M. J. Hytch, E. Snoeck, and R. Kilaas, *Ultramicroscopy*, vol. 74, pp. 131–146, 1998.
[23] L.-N. Tong, F. Matthes, M. Müller, C. M. Schneider, and C.-G. Lee, *Phys. Rev. B*, vol. 77, p. 064421, 2008.
[24] P. Turban, L. Hennet, and S. Andrieu, *Surf. Sci.*, vol. 446, p. 241, 2000.